African Journal of Pharmaceutical Research & Development

Vol. 11 No.2; pp. 074-087 (2019)

SURFACE-MODIFIED BEESWAX-BASED NANO-LIPOGELS AS POTENTIAL DRUG DELIVERY SYSTEM: PRELIMINARY PHYSICOCHEMICAL CHARACTERIZATION

FRANKLIN CHIMAOBI KENECHUKWU[1,*], MUMUNI AUDU MOMOH[1], CHUKWUEBUKA HARFORD OZOUDE[2], ANTHONY AMAECHI ATTAMA[1], EMMANUEL CHINEDUM IBEZIM[1]

1. Drug Delivery and Nanomedicines Research Group, Department of Pharmaceutics, University of Nigeria, Nsukka 410001, Enugu State, Nigeria.
2. Department of Pharmaceutics and Pharmaceutical Technology, Faculty of Pharmacy, University of Lagos, Lagos State, Nigeria.

ABSTRACT

Surface-modification is a promising tool in drug delivery. The aim of this study was to prepare and characterize surface-modified nano-lipogels as potential drug delivery system. The nanotool was developed based on mineral fat (beeswax) and surface-modifier [Phospholipon ® 90H (P90H)] and investigated for enhanced physicochemical performance of miconazole nitrate (MN), a poorly water-soluble imidazole antifungal. Differential scanning calorimetry analysis revealed the amorphous nature of the optimized solidified reverse micellar solution (SRMS) containing rational ratio of beeswax and P90H (3:7) used in preparing the solid lipid nano-dispersion (SLN) as well as MN-loaded SRMS. The SLN prepared by high-shear hot homogenization (melt-emulsification) showed irregular and spherical nanoparticles, had low polydispersity indices, with average particle size in the range of 204.0 ± 2.9 to 263.0 ± 7.1 nm. The developed lipid nano-lipogels were spreadable and viscoelastic. Fourier transform infra-red (FT-IR) spectra indicated components compatibility. This study has shown that phospholipid-modified beeswax-based lipid nano-lipogels could be employed as potential drug delivery system to enhance the physicochemical performance of MN.

KEYWORDS: **Physicochemical characterization; Drug delivery system; Solid lipid nano-dispersions (SLNs); Nano-lipogels; Phospholipon® 90H (P90H); Beeswax; Solidified reverse micellar solution (SRMS).**

INTRODUCTION

Several strategies have been explored to prolong the contact of drugs with the oral mucosa, including the use of nanotechnology and mucoadhesives to prolong the residence time of the dosage form [1]. These systems have several remarkable benefits including localized drug delivery to enhance efficacy of incorporated drugs [2, 3], modification of the permeability of mucosal tissue or membranes and hence facilitated adsorption of macromolecules, e.g., peptides, prolongation of the residence time of the dosage form at the site of application, hence reduction in dosage frequency and increased patient compliance [4, 5]. Nanoparticulate mucoadhesive drug delivery systems (MDDS) have been employed in various ways to deliver many drugs and bioactives [6, 7], including antifungal drugs [8]. Furthermore, lipid-based drug delivery systems (LBDDS), which are accepted, proven, commercially viable strategies for formulating challenging pharmaceutical molecules, could be tailored to improve MN delivery via the oral mucosa owing to their advantages such as high stability, high carrier capacity, among others [9, 10]. In the past few years, our research group has reported improved delivery of several bioactives and drugs especially gentamicin and antimalarial drugs by formulation as solid lipid microparticles (SLMs)

*Corresponding author: frankline.kenechukwu@unn.edu.ng; +2348038362638

and solid lipid nanoparticles (SLNs) using the promising technology of solidified reverse micellar systems (SRMS) [11-15], including beeswax-based SLMs [16]. However, the most recent lipid-based drug delivery approach adopted so far to enhance the delivery of drugs, and minimize toxicity effects is the incorporation of the drug into inert lipid nanoparticles in a gel base [17]. These systems are mucoadhesive and have potential for localized treatment of infections [17]. Thus, to tackle the problem of resistance to MN for effective treatment of OPC, a more patient-friendly dosage forms such as SRMS-based nanoparticulate MDDS which would improve patient compliance to course of treatment while preventing drug resistance due to non-compliance would be needed to selectively localize the drug at pre-selected target of *C. albicans* and diseased oral mucosa in therapeutic concentration, while restricting its access to non-target areas, thus maximizing the effectiveness of the drug and minimizing its side effects.That is to say, nano-lipogels made up of lipid nanoparticles in a gel base [17] could be developed using beeswax and phospholipids, adopting the promising technology of solidified reverse micellar systems (SRMS), and exploited as potential oromucosal formulation to target MN to the oromucosal layers for effective OPC treatment.

In this study, SRMS consisting of Phospholipon® 90H (a phospholipid) and beeswax (a hard fat) was prepared, characterized and employed to formulate and evaluate phospholipid-modified beeswax-based mucoadhesive nano-lipogels for prolonged localized oromucosal delivery of MN. Phospholipids are attractive delivery vehicle forming a building block of some nanoparticles for some drug molecules to enhance the absorption across lipid-rich biological barriers and increase efficacy. As an amphipathic molecule, phospholipids possess a positively charged head group and two neutrally charged tail groups, a rare molecular characteristic that renders phospholipids miscible in both water and lipid and able to facilitate the crossing of the cell-membrane barrier [13, 18]. Therefore, the exploration of an effective phospholipid-modified nanoparticulate drug delivery system would prolong the delivery of MN and improve patient compliance to treatment which invariably would provide the following advantages: smaller drug doses with fewer and/or no side effects, longer residence time (less frequent dosing) with more target specificity and controlled release as well as improved compliance. Meanwhile, there is paucity of information on the use of phospholipid-modified beeswax-based (SRMS-based) mucoadhesive nano-lipogels for improved controlled oropharyngeal delivery of anticandidal drugs. Consequently, the aim of this study was to prepare and evaluate phospholipid-modified beeswax-based mucoadhesive lipid nano-lipogels for prolonged localized oromucosal delivery of MN.

MATERIALS AND METHOD

Materials

The pure sample of miconazole nitrate used was purchased from Gutic Biosciences Limited, India. Phospholipon® 90H (P90H) was kindly provided by Phospholipid GmbH (Köln, Germany). Other materials include methanol and ethanol (Sigma Aldrich, USA), sorbic acid (Foodchem Int. Co., China), Polysorbate® 80 (Tween® 80) (Merck KGaA, Darmstadt, Germany), beeswax (white) (Ph. Eur. Carl Roth GmbH + Co. KG Karlsruhe, Germany), Polycarbophil (Noveon®) (Lubrizol Corporation, Ohio, USA) and distilled water (Lion water Ltd., University of Nigeria, Nsukka, Nigeria). The brand of commercially available miconazole nitrate oral gel used was Daktarin® oral gel (McNeil Products Ltd., Maidenhead, Berkshire, SL6 3UG, UK). All other chemicals and reagents used were analytical grade and obtained commercially.

Preparation of plain and drug-loaded lipid matrices

The lipid matrix for solid lipid nanoparticles (SLNs) formulation was prepared by fusion using Phospholipon ® 90H and white beeswax (at 3:7 ratio). The lipids were weighed, melted together at 70 °C in a temperature-regulated oil bath and stirred until a homogenous, transparent melt of the solidified reverse micellar solution (SRMS) was obtained. The homogenous mixture of the SRMS was then stirred at room temperature until solidification. The SRMS was stored in airtight and moisture resistant glass bottles in the refrigerator until used. Miconazole nitrate-loaded lipid matrix was prepared by fusion as described before using 4.0 g of the lipid matrix and 0.4 g of MN.

Characterization of plain and MN-loaded lipid matrices

The prepared plain and MN-loaded lipid matrices were characterized by differential scanning calorimetry (DSC). Thermal properties of the lipid matrix and the individual lipids were determined using a calorimeter (Netzsch DSC 204 F1, Germany). About 5 mg of each sample was weighed into an aluminum pan, hermetically sealed and the

thermal behaviour determined in the range of 20 – 250 °C at a heating rate of 5 °C/min. The temperature was held at 80 °C for 10 min and thereafter, cooled at the rate of 5 to 10 °C/min. Baselines were determined using an empty pan, and all the thermograms were baseline-corrected.

Preparation of solid lipid nanoparticles (SLNs)

Miconazole nitrate-loaded SLNs were prepared using the drug, lipid matrix, Polysorbate® 80 (Tween® 80) (mobile surfactant), sorbitol (cryoprotectant) and distilled water (vehicle) by the high shear hot emulsification-homogenization method [15]. Briefly, specified quantity of each lipid matrix (5 %w/w of the SLNs formulation) was placed in glass beaker and melted at 80 ˚C in a temperature-regulated oil bath on a hot-plate magnetic stirrer assembly and increasing amount of miconazole nitrate (0.25, 0.5 and 1.0 %w/w) was added to the melted lipid matrix. At the same time, an aqueous surfactant solution consisting of sorbitol (4 %w/w) and Polysorbate® 80 (2 %w/w) were prepared in a separate beaker and heated at the same temperature. The hot aqueous surfactant phase was then transferred into the hot lipid phase and thereafter homogenized using an Ultra-Turrax (T25 Basic IKA-Werke, Staufen, Germany) at 15,000 rpm for 20 min, and allowed to re-crystallize at room temperature. Unloaded SLN formulations were also prepared to serve as control. In summary, the SLNs contain lipid matrix (5.0 %w/w), Polysorbate® 80 (2.0 %w/w), sorbitol (4.0 %w/w), MN (0, 0.25, 0.5, 1.0 %w/w) and distilled water (q.s. to 100.0 %w/w).

Determination of surface charge, particle size and polydispersity indices

The zeta potential of SLNs formulations was determined via electrophoretic mobility measurements using a Zetasizer Nano-ZS (Malvern Instruments, UK). The mean diameter and polydispersity index of both plain and drug-loaded SLNs were also measured using a Zetasizer Nano-ZS (Malvern Instruments, UK). All samples were diluted with a fixed amount of deionized water to obtain a suitable scattering intensity, before photon correlation spectroscopic (PCS) analysis.

Scanning electron microscopy (SEM)

The morphological characteristics of the SLNs were determined using a scanning electron microscope (JEOL-JSM-6 360, Japan). One drop of sample was placed on a slide and excess water was left to dry at room temperature. The slide was attached to the specimen holder using double coated adhesive tape and gold coating under vacuum using a sputter coater (Model JFC-1100, JEOL, Japan) for 10 min, and then investigated at 20 kV.

Fourier transform infra-red (FT-IR) spectroscopy

FT-IR spectroscopic analysis was carried out using a Shimadzu FT-IR 8300 Spectrophotometer (Shimadzu, Tokyo, Japan). The potassium bromate (KBr) plate used for the study was cleaned with a tri-solvent (acetone–toluene–methanol at 3:1:1 ratio) mixture for baseline scanning. A 0.1 ml volume of each batch of the SLMs was mixed with 0.1 ml nujul diluent. The solution was introduced into the potassium bromate (KBr) plate and compressed into pellets, each of which was placed in the light path and the spectrum obtained. The mixture was ground into a fine powder using an agate mortar before compressing into a disc. Each disc was scanned at a resolution of 4 cm^{-1} over a wave number region of 400 - 4000 cm^{-1} using FT-IR spectrophotometer (Model 500, Buck Scientific, USA) coupled to a computer with Omnic analysis software. The characteristic peaks of infra-red transmission spectra were recorded.

Preparation of mucoadhesive SRMS-based nano-lipogels

The mucoadhesive SRMS-based nano-lipogels were prepared using the mucoadhesive agent (Polycarbophil®, PCP) and other relevant ingredients (glycerol, sorbic acid and distilled water) in addition to the SLN formulations by dispersion method [19]. Briefly, PCP (1.0 %w/w) was dispersed in 30 ml of distilled water in a glass beaker. After an overnight solubilization, glycerol (3.0 %w/w), sorbic acid (0.02 %w/w) and SLNs from each batch (20 ml) (to yield 0, 0.05, 0.10, 0.20 %w/w MN) were incorporated into the PCP aqueous dispersion, with continuous stirring after each addition. In each case, the system was made up to 100.0 %w/w with distilled water and stirred vigorously for 2 h until a homogenous consistent gel was formed. The formulation was then poured into an ointment jar and the pH was raised to 6.8 by drop-wise addition of 0.5 M NaOH.

Spreadability determination

The spreadability of the gel formulations was determined following a reported procedure [20]. A

0.5 g quantity of the gel formulation was sandwiched between two glass slides: a lower calibrated slide marked into 5 cm spaces and an unmarked upper slide. Different weights of 50, 100, 200 and 300 g were placed over the upper slide at 1 min intervals. The diameter occupied by the spreading gel was finally measured to determine the area of spread (length x width). The sample weight was fixed in order to have same assay for all the samples and to limit the glass from sliding.

FT-IR spectroscopic analysis of the mucoadhesive SRMS-based nano-lipogels

FT-IR spectroscopic analysis was carried out using a Shimadzu FT-IR 8300 Spectrophotometer. All aspects of the protocol involved in the FT-IR spectroscopic analysis were the same as those outlined above.

Dynamic oscillatory rheometry on optimized mucoadhesive SRMS-based nano-lipogels

The optimized gel formulation was characterized rheologically using HAAKE ThermoRheoWin rheometer (Thermo Fisher Scientific, Schwerte, Germany). Continuous shear analysis of each formulation was performed at 20 °C ± 0.1°C, in flow mode, and in conjunction with parallel steel plate geometry (diameter 40 mm) and gap of 0.3 mm. Samples were carefully applied to the lower plate of instrument, ensuring that formulation shearing was minimized and allowed to equilibrate for at least 1 min prior to analysis. Oscillatory analysis of each formulation under examination was performed after determination of its linear viscoelastic region (LVER) at 20 °C ± 0.1°C, where stress was directly proportional to strain and the storage modulus remained constant. Amplitude sweep analysis was performed at constant frequency following application of stress within the range of 0.1 – 200 Pa and standard gap size was 0.3 mm for each sample. Storage/elastic modulus (G´) and loss/viscous modulus (G´´), the dynamic/complex viscosity (η^*), the phase angle (δ) and loss tangent (tan δ) were determined [19, 21].

Data and statistical analysis

All experiments were performed in replicates for validity of statistical analysis. Results were expressed as mean ± SD. Student's t-test were performed on the data sets generated using Statistical Package for Social Sciences (SPSS) software, version 12 (Chicago, IL). Differences were considered significant at $p < 0.05$.

RESULTS

Thermal properties

The thermal properties of phospholipid-modified beeswax-based lipid matrix are shown in Fig. 1A. The melting endotherm of beeswax was 73. °C with an enthalpy of - 55.3 mW/mg [Fig. 1A(a)]. The DSC profile of P90H showed a sharp endothermic peak corresponding to melting at 122.10 °C [Fig. 1A(b)]. However, when the lipid was used in the formulation of SRMS matrix, the SRMS 7:3 of beeswax and P90H gave a DSC value of 88.6 °C and an enthalpy of - 32.5 mW/mg [Fig. 1A(c)].
Results of drug-lipid compatibility and crystallization studies carried out based on DSC are presented in Fig. 1B(a)-1B(c). DSC result of MN showed a melting peak of 188.0 °C with corresponding enthalpy of -15.69 mW/mg. Partial recrystallization occurs after second order transition at 202.4 C° [Fig. 1B(a)]. The DSC results of MN-loaded lipid matrix showed different melting peak and thermal property as depicted in Fig. 1B(c). MN-loaded lipid matrix based on beeswax and P90H [Fig. 1B(c)] showed a melting peak of 110.0 °C with an enthalpy of - 32.89 mW/mg. MN-loaded lipid matrix gave lower melting point than pure MN powder.

Particles properties of the SLNs

Fig. 2 with Table 1 shows the particle properties of the SLNs. Photon correlation spectroscopy (PCS) data showed that the mean particle size of MN-free SLNs was 263.0 ± 7.1 nm, while MN-loaded SLNs containing 0.25, 0.5 and 1.0 %w/w of MN had particle sizes of 262.4 ± 13.0, 243.5 ± 6.8 and 204.0 ± 2.9 nm (for beeswax-based SLNs), respectively. Similarly, the polydispersity index of MN-free SLNs was 0.274 ± 0.04, while MN-loaded SLNs containing 0.25, 0.5 and 1.0 %w/w of MN had polydispersity indices of 0.239 ±0.01, 0.248 ± 0.06 and 0.238 ± 0.02, respectively. Meanwhile all particles were within nanometer size ranges as expected for well-formed SLNs (Fig. 2a-2d). The zeta potential (ZP) values obtained for the formulations were -32.9 ± 1.7 mV for drug-free SLNs and -36.7 ± 2.5, -39.8 ± 0.9 and -40.1 ± 1.3 mV for drug-loaded SLNs containing, respectively, 0.25, 0.5 and 1.0 %w/w of MN].

Scanning electron micrograph of SLN

The shape and surface morphology of SLNs formulations in aqueous systems were studied by SEM and the micrograph of the SLNs (selected formulation) is presented in Fig. 3. The micrograph of the SLNs showed that the particles contained a mixture of spherical and non-spherical (anisometric) shapes with similar sizes spread all over the formulation, corresponding to the somewhat narrow distribution of droplets earlier observed in the formulations.

Compatibility by FT-IR spectroscopic analysis of the SLNs

The FT-IR spectrum of pure MN sample (not presented) showed principal characteristic absorption bands at 2494 cm^{-1} (N-H stretching of benzene ring), 3205 cm^{-1} (OH group), 2895 cm^{-1} (C-H stretching of benzene ring), 2323 cm^{-1} (C=N stretching), 1732 cm^{-1} (carbonyl compound: CHO), 1600 cm^{-1} (conjugated α,β-unsaturated C=C bond in benzene ring), 1410 cm^{-1} (NO_2: nitro group), 1283 (C-O ester in benzene ring), 859 cm^{-1} and 730 cm^{-1} (aromatic C-Cl deformation). The FT-IR spectra of MN-loaded SLNs are shown in Fig. 4a. The FT-IR spectrum of batch F_1 showed principal characteristic absorption bands of MN at 3940 cm^{-1}, 3786 cm^{-1} and 3508 cm^{-1} (N-H stretching), 3230 cm^{-1} and 3080 cm^{-1} (OH group), 2894 cm^{-1} (C-H stretching), 2296 cm^{-1} and 2188 cm^{-1} (C=N stretching), 1377 cm^{-1} (NO_2: nitro group), 1289 cm^{-1} and 1011 cm^{-1} (C-O ester in benzene ring), 883 cm^{-1} and 536 cm^{-1} (aromatic C-Cl deformation). The FT-IR spectrum of batch F_2 showed principal characteristic absorption bands of MN at 3909 cm^{-1}, 3755 cm^{-1} and 3508 cm^{-1} (N-H stretching), 3141 cm^{-1} and 3045 cm^{-1} (OH group), 2952 cm^{-1} and 2829 cm^{-1} (C-H stretching), 2207 cm^{-1} (C=N stretching), 1578 cm^{-1} and 1377 cm^{-1} (NO_2: nitro group), 1169 cm^{-1} (C-O ester in benzene ring) and 702 cm^{-1} (aromatic C-Cl deformation). The FT-IR spectrum of batch F_3 showed principal characteristic absorption bands of MN at 3786 cm^{-1} and 3693 cm^{-1} (N-H stretching), 3446 cm^{-1}, 3292 cm^{-1} and 3014 cm^{-1} (OH group), 2860 cm^{-1} (C-H stretching), 2242 cm^{-1} and 2153 cm^{-1} (C=N stretching), 1412 cm^{-1} and 1319 cm^{-1} (NO_2: nitro group), 1254 cm^{-1} and 1130 cm^{-1} (C-O ester in benzene ring) and 794 (aromatic C-Cl deformation).

Spreadability of the nano-lipogels

Spreadability results (Fig. 5) generally showed that the most spreadable was the drug-loaded mucoadhesive SRMS-based nano-lipogels containing the highest amount of MN (1.0 %w/w) (batch F_3 Gel) followed by mucoadhesive SRMS-based nano-lipogels without drug (batch F_0 Gel) and thirdly by batch F_1 Gel and lastly by batch F_2 Gel containing, respectively, 0.25 and 0.5 %w/w of MN (Fig. 5). Furthermore, there was load (weight)-dependent increase (300 g > 200 g >100 g > 50 g) in areas of spread across all batches.

Compatibility by FT-IR spectroscopic analysis of the mucoadhesive SRMS-based nano-lipogels

The FT-IR spectra of MN showed principal characteristic absorption bands of MN previously described above. The FT-IR spectra of MN-loaded mucoadhesive SRMS-based nano-lipogels are shown in Fig.4b. The FT-IR spectrum of batch F_1 Gel showed principal characteristic absorption bands of MN at 3601 cm^{-1} (N-H stretching), 3141 cm^{-1} and 3033 cm^{-1} (OH group), 2805 cm^{-1} (C-H stretching), 2149 cm^{-1} (C=N stretching), 1566 cm^{-1}, 1470 cm^{-1} and 1319 cm^{-1} (NO_2: nitro group), 1227 cm^{-1} and 1073 cm^{-1} (C-O ester in benzene ring), 949 cm^{-1}, 856 cm^{-1}, 702 cm^{-1} and 578 cm^{-1} (aromatic C-Cl deformation). The FT-IR spectrum of batch F_2 Gel showed principal characteristic absorption bands of MN at 3882 cm^{-1}, 3782 cm^{-1} and 3632 cm^{-1} (N-H stretching), 3153 cm^{-1} and 3022 cm^{-1} (OH group), 2890 cm^{-1} (C-H stretching), 2273 cm^{-1} and 2153 cm^{-1} (C=N stretching), 1628 cm^{-1} (conjugated α,β-unsaturated C=C bond in benzene ring), 1462 cm^{-1} (NO_2: nitro group), 1289 cm^{-1}, 1231 cm^{-1}, 1165 cm^{-1} and 1099 cm^{-1} (C-O ester in benzene ring), 829 cm^{-1}, 702 cm^{-1} and 682 cm^{-1} (aromatic C-Cl deformation). The FT-IR spectrum of batch F_3 Gel showed principal characteristic absorption bands of MN at 3817 cm^{-1}, 3759 cm^{-1}, 3693 cm^{-1} and 3018 cm^{-1} (OH group), 2952 cm^{-1} (C-H stretching), 2153 cm^{-1} (C=N stretching), 1725 cm^{-1} (CHO: carbonyl group), 1659 cm^{-1} (conjugated α,β-unsaturated C=C bond in benzene ring), 1335 cm^{-1} (NO_2: nitro group), 1223 cm^{-1} (C-O ester in benzene ring), 922 cm^{-1}, 794 cm^{-1} and 517 cm^{-1} (aromatic C-Cl deformation).

Dynamic rheological properties

Fig. 6a shows the rheological properties of optimized mucoadhesive SRMS-based nano-lipogel (batch F_2 Gel) whereas the result of effect of dynamic viscosity on the shear stress is shown in Fig. 6b for batch F_2 Gel.

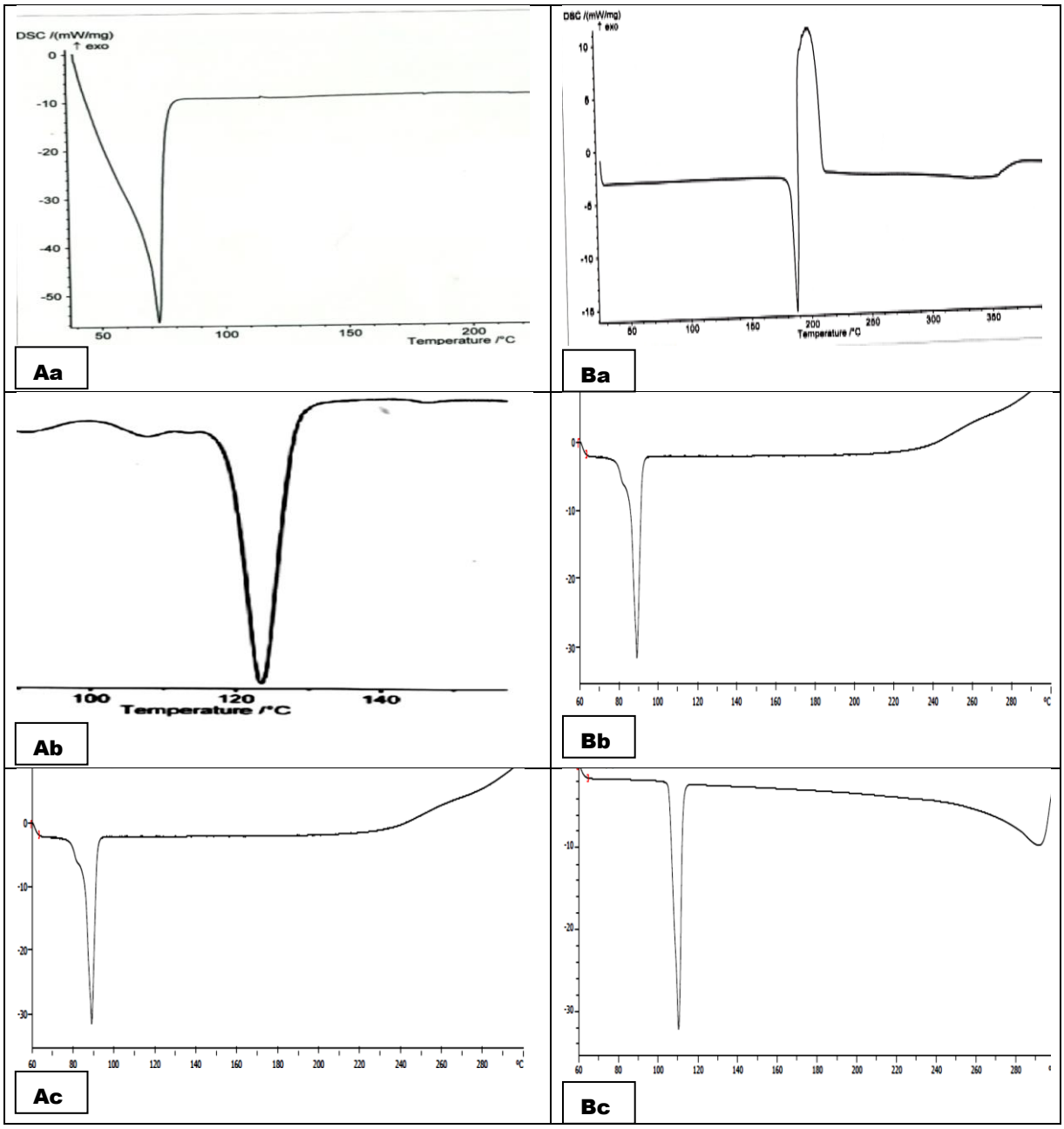

Fig. 1: Thermal properties showing (A) DSC thermograms of (a) beeswax, (b) Phospholipon® 90H (P90H) and (c) lipid matrix based on beeswax and P90H, (B) DSC thermograms of (a) MN, (b) lipid matrix based on beeswax and Phospholipon 90H (7:3) and (c) MN-loaded structured lipid matrix.

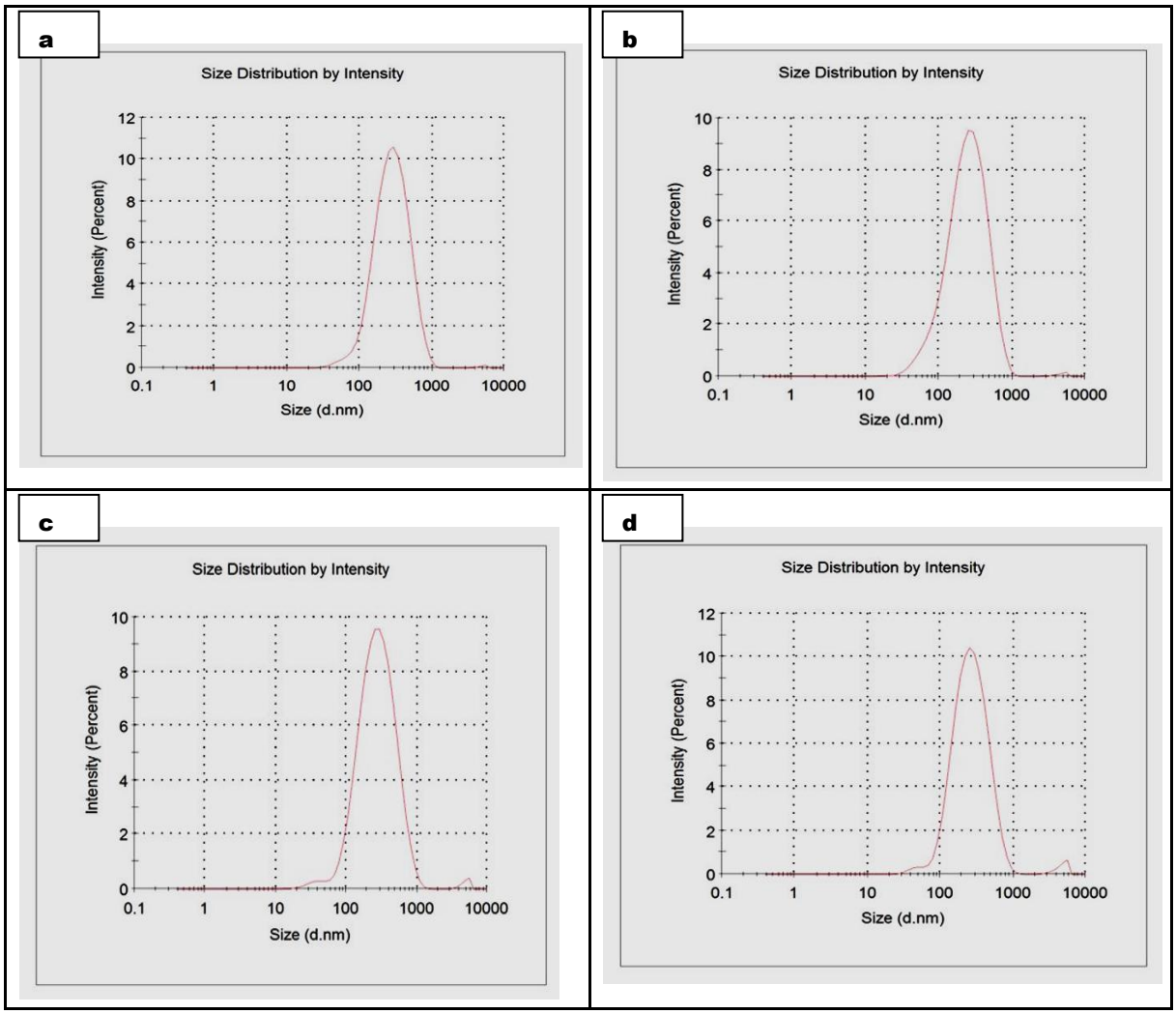

Fig. 2: Size distribution of SRMS-based SLNs (a) unloaded SLN based on beeswax and P90H (F_0) (b) 0.25 %w/w MN-loaded SLN based on beeswax and P90H (F_1) (c) 0.5 %w/w MN-loaded SLN based on beeswax and P90H (F_2) and (d) 1.0 %w/w MN-loaded SLN based on beeswax and P90H (F_3).
Key: F_1, F_2 and F_3 are SRMS-based SLNs containing increasing concentrations (0.25, 0.5 and 1.0 %w/w, respectively) of miconazole nitrate while S_0 is plain or unloaded SRMS-based SLNs.

Fig. 3: Scanning electron micrograph of MN-loaded SRMS-based SLNs (representative batch).

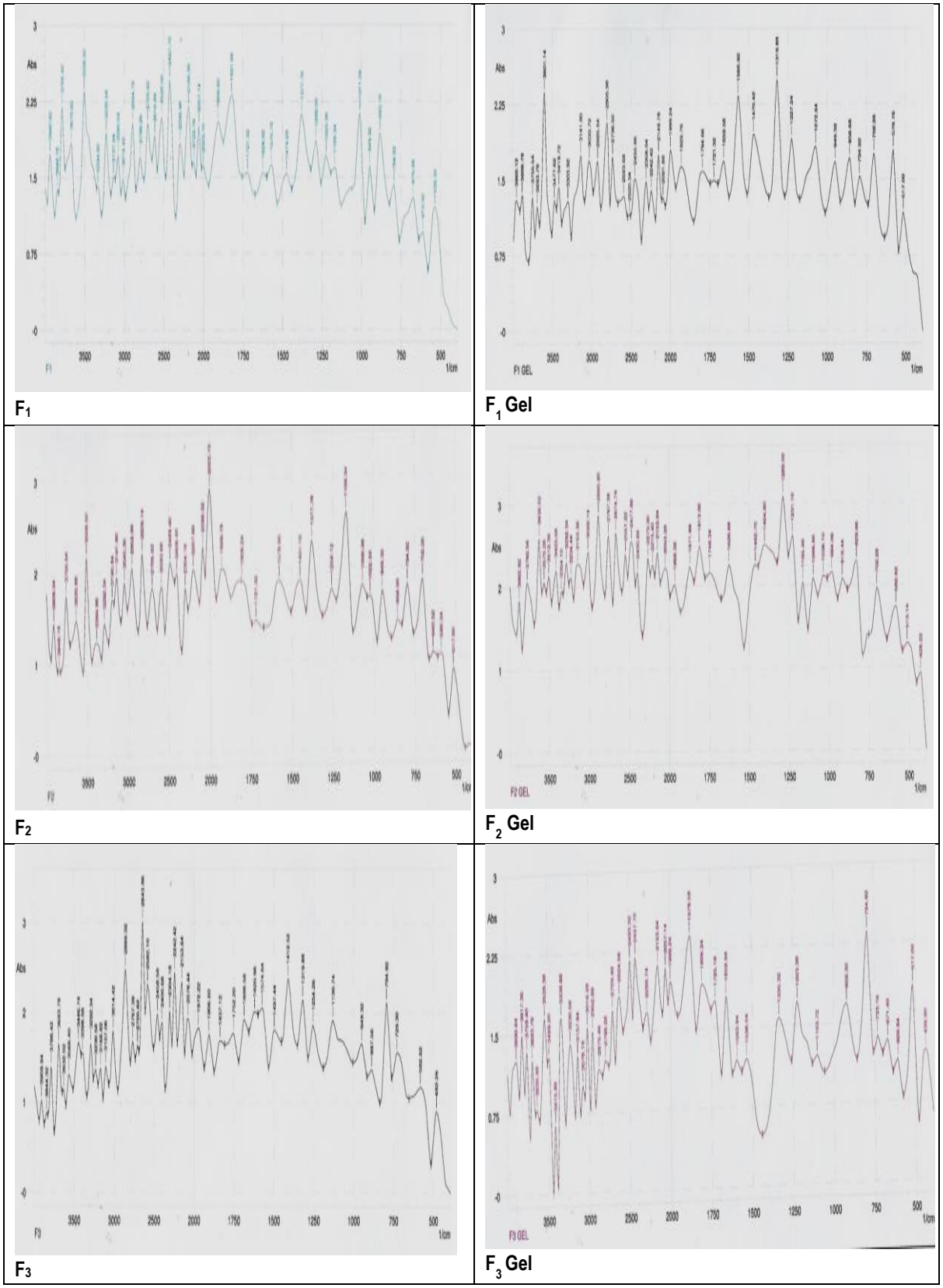

F_1 **F_1 Gel**

F_2 **F_2 Gel**

F_3 **F_3 Gel**

Fig. 4: FT-IR spectra of (a) MN-loaded SRMS-based SLNs and (b) MN-loaded mucoadhesive SRM-based nano-lipogels.

Key: F_1 - 0.25 %w/w MN-loaded SRMS-based SLN, F_2 - 0.5 %w/w MN-loaded SRMS-based SLN, F_3 - 1.0 %w/w MN-loaded SRMS-based SLN, F_1 Gel, F_2 Gel and F_3 Gel are mucoadhesive SRMS-based nano-lipogels containing increasing concentrations (0.25, 0.5 and 1.0 w/w, respectively) of miconazole nitrate.

Table 1: Some physicochemical properties of the solid lipid nanoparticles (SLNs)

Sample	Z-Av. (nm)	PDI	ZP (mV)	EE (%)	DL (%)
F_0	263.0 ± 7.1	0.274 ± 0.04	-32.9 ± 1.7	-	-
F_1	262.4 ± 13.0	0.239 ± 0.01	-36.7 ± 2.5	44.50 ± 1.99	12.49 ± 3.05
F_2	243.5 ± 6.8	0.248 ± 0.06	-39.8 ± 0.9	58.87 ± 3.56	18.24 ± 2.99
F_3	204.0 ± 2.9	0.238 ± 0.02	-40.1 ± 1.3	36.23 ± 2.01	9.82 ± 0.67

Key: Z-Av means average particle size; PDI means polydispersity indices; ZP means zeta potential; EE means encapsulation efficiency; DL means drug loading; F_0- F_3 are beeswax-based SLNs; F_1, F_2 and F_3 contain increasing concentrations (0.25, 0.5 and 1.0 %w/w, respectively) of miconazole nitrate, while F_0 is plain or unloaded SLNs.

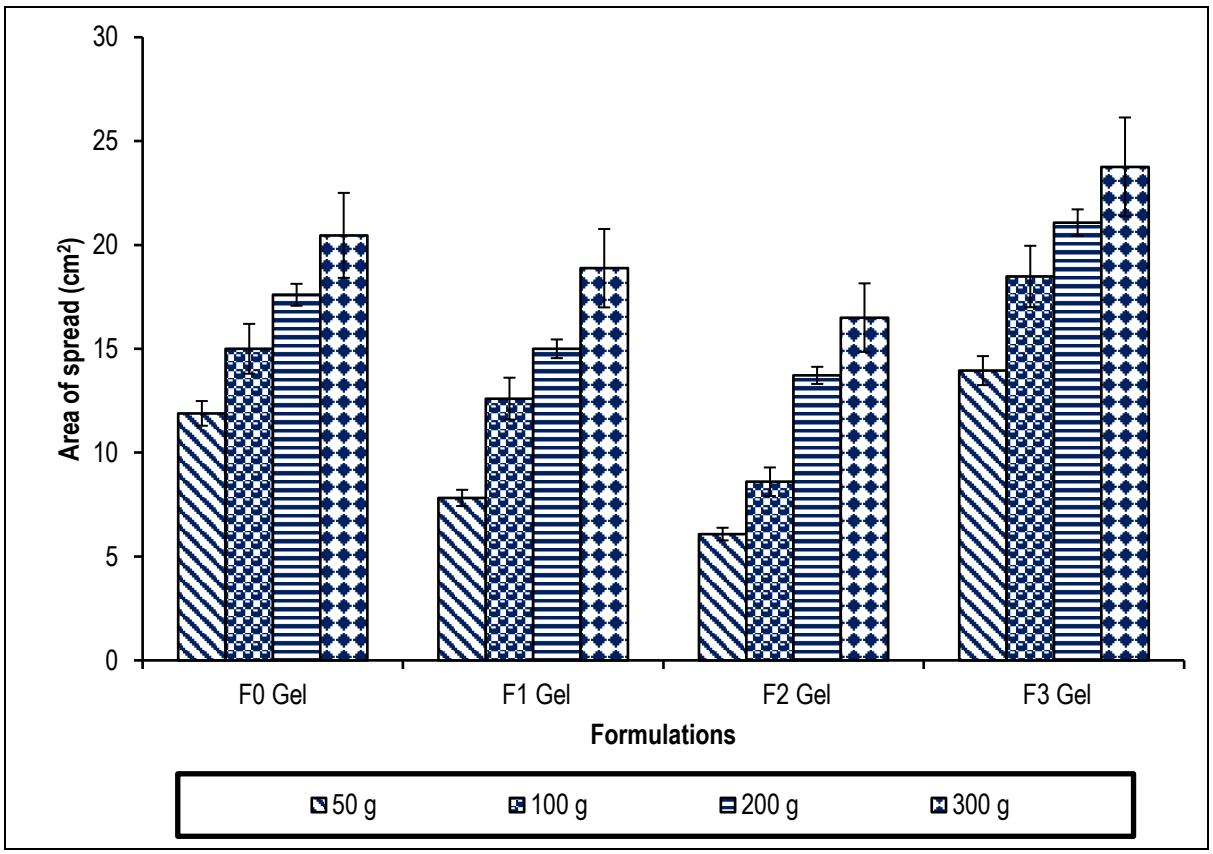

Fig. 5: Spreadability of mucoadhesive SRMS-based nano-lipogels.

Key: F_1 Gel, F_2 Gel and F_3 Gel are mucoadhesive SRMS-based nano-lipogels containing increasing concentrations (0.25, 0.5 and 1.0 %w/w, respectively) of miconazole nitrate while S_0 Gel is plain or unloaded mucoadhesive SRMS-based nano-lipogels.

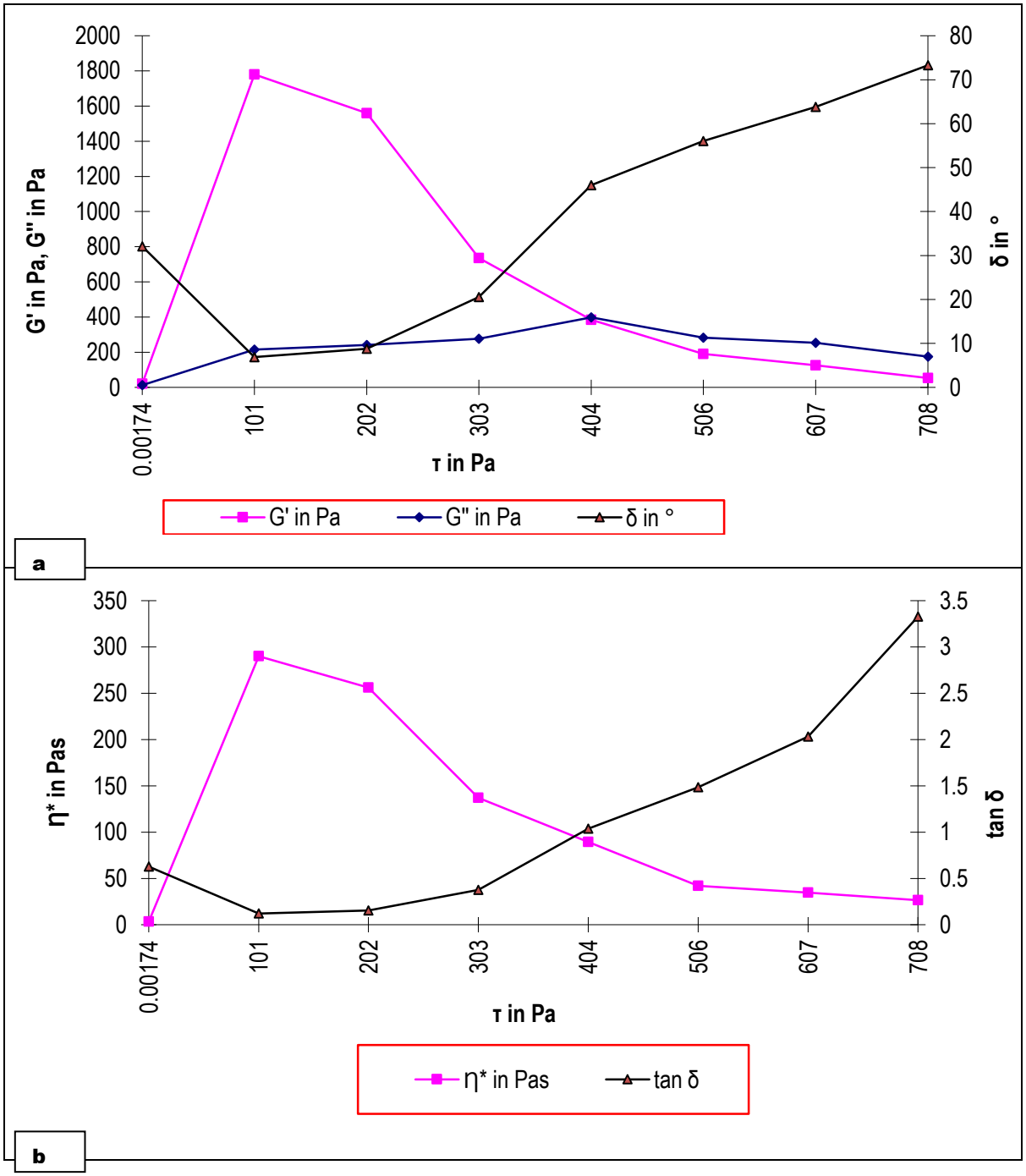

Fig. 6: (a) Rheogram showing the rheological properties of optimized MN-loaded SRMS-based mucoadhesive nano-lipogels (S_2 Gel), (b) Rheogram showing the effect of oscillatory stress on the dynamic viscosity and loss tangent of optimized MN-loaded SRMS-based mucoadhesive nano-lipogels (S_2 Gel).

Key: F_1 Gel, F_2 Gel and F_3 Gel are mucoadhesive SRMS-based nano-lipogels containing increasing concentrations (0.25, 0.5 and 1.0 %w/w, respectively) of miconazole nitrate while Daktarin® oral gel is a commercially available gel containing 2.0 %w/w miconazole nitrate; G' - Storage (elastic) modulus, G" - Loss (viscous) modulus, τ - Oscillatory stress, δ - Phase angle, η* - Dynamic (complex) viscosity and tan δ - Loss tangent.

DISCUSSION

The DSC results show that the blend of beeswax with P90H produced matrix with low enthalpy and clearly showed the interaction of the lipid mixture. Thus, the SRMS 7:3 of BW and P90H may have generated an imperfect matrix resulting from distortion of crystal arrangement of the bulk lipid after melting and solidification. This distortion of the lipid crystal may serve as an advantage in drug encapsulation, entrapment and enhanced drug tolerability [11, 22]. Partial recrystallization, which occurred after second order transition in the DSC thermogram of MN, is the characteristic feature of MN [23]. The DSC thermogram of MN showed sharp endothermic peak which revealed the crystalline nature and purity of the drug when compared with already reported characteristics of MN. Since decrease in melting point values indicate less ordered crystal structures [11, 20], it follows that MN-loaded lipid matrix based on beeswax and P90H was less crystalline than MN and equally showed that MN existed in amorphous form in the lipid matrix encapsulating the drug; the drug was properly solubilized in lipid matrix based on beeswax and P90H, consistent with previous reports [23-25]. Furthermore, the thermograms of MN-loaded lipid matrix showed the melting peak of the carrier matrix but without the drug peak, indicating that the drug may have changed from crystalline to its amorphous structure. The loading of MN into the structured lipid matrix also resulted in a reduction of enthalpy and crystallinity. The thermal behavior of a lipid matrix usually changes in the presence of other substances such that the melting temperature and changes in enthalpy depend on the nature of interaction between the constituents [15]. The presence of P90H reduced the crystallinity of beeswax, and this was observed as lower enthalpy and melting point of the lipid matrix. Lower enthalpy and melting points could possibly cause retention of an entrapped drug over time [11]. Also, they may imply imperfect lattices with pockets of spaces that can accommodate drugs [20]. The endothermal transition of the lipid matrix was very broad, indicating different modifications of the complex lipid matrix composition. The mixture of the drug and the lipid matrix did not show any transition of the drug in the thermogram, indicating either existence in an amorphous form or in a solubilized form.

Particle characterization of SLNs is essential to ensure the production of stable product of suitable quality. Physical stability and cellular uptake of nanoparticles are affected by particle size [14, 25]. Size distribution is affected by stirring rate, temperature, type and amounts of polymers and/or lipids as well as viscosity of the continuous phase [9, 24]. Drug loading resulted to an insignificant ($p > 0.05$) decrease in both the mean particle size and polydispersity indices of the SLNs. The reason for this effect is unknown but may be related to increased solubilization of the lipophilic drug in the core of the lipid matrix as well as formation of other structures such as mixed nano-micelles within the SLN dispersions [25-27]. The polydispersity indices of MN-loaded SLNs indicated low PDI and narrow distribution that would result in physical stability of the formulations, with little or no potential for particle growth [25]. This is especially true as the particle size analysis was carried out after more than one month of preparation of the SLNs and storage at ambient temperature (28.0 ± 3.0 °C). The stability of the formulations was also confirmed by the zeta potential or surface charge measurement, which showed that the values were above |30 mV|, as those recommended for aqueous nanoparticle dispersions to be considered stable [9, 14]. This suggests that the surface properties of the particles in all formulations were not altered during the 1-month storage period (before the analysis).

Regarding the morphology of the SLNs, it should be noted that it is not possible to determine the particle size distribution in a freeze-fractured preparation because the matrix lipid does not recrystallize under the condition, hence, the orientation of the SLN droplets as circular or somewhat cuboidal, whitish structures when viewed edge-on. The micrograph also showed that there was no droplet aggregation in the formulations, indicative of physical stability. However, the slight aggregation of the SLNs could be due to insufficient drying time of the sample during sample preparation prior to SEM analysis. The shape of solid lipid nanocarriers has been reported to be dependent on the purity of the lipids used and particles prepared from highly pure lipids are usually more cuboidal in nature, whereas those obtained using chemically polydispersed lipids are typically spherical [1]. The lipid matrix used in this study consisted of a mixture of solid lipids (beeswax and P90H) and all of them are highly purified (synthetic) lipids, which suggests that the lipid matrices were chemically polydispersed as well as highly pure. Although it is expected that only spherical particles would be present in all formulations, it should also be realized that the nature of the lipid matrices used could determine the shape of the particles. In particular, previous studies have established that the shapes of solid lipid nanocarriers might be spherical or non-spherical [24]. The developed SLNs comprise of spherical and

non-spherical particles. However, the degree of crystallinity and nature of particles in lipid nanoparticulate formulations need to be further confirmed by other analytical techniques [9, 14].

Overall FT-IR results suggest absence of any incompatibility between the drug and excipients used in the formulation of the SLNs and mucoadhesive SRMS-based nano-lipogels as well as existence of the drug in its native form [23].

Meanwhile, owing to its nature Polycarbophil® (PCP) would impart the flow-like honey (high spreadability) property on the semi-solid formulation, in perfect agreement with earlier report [19]. Hence, the good spreadability of all the mucoadhesive SRMS-based nano-lipogel formulations with consistent increase in weight, in line with previous report [20] thus necessitating further development of the latter as oromucosal dosage form. The results showed that the mucoadhesive SRMS-based nano-lipogel formulations had excellent measure of spreadability. Oromucosal gel preparations that have good spreadability encourage patient compliance [1, 4, 8, 28].

The results of rheological studies indicate that at low shear stresses, the storage/elastic modulus (G') was always greater than loss/viscous modulus (G"), indicating that the material exhibited “solid-like” or “gel-like” properties. With further increase in shear stress, G' significantly ($P < 0.05$) reduced, while G" increased in general, but G' was still greater than G" until the yield stress (cross-over point) was reached. Yield stress has been defined as the shear stress at which its corresponding storage modulus is less than 95 % of the average value from the first three detected storage moduli within the viscoelastic region, which represents initial gel elasticity [19]. The yield stresses of the optimized formulation indicated that the optimized mucoadhesive SRMS-based nano-lipogel deformed upon addition of stress causing it to shear-thin. The cross-over of G' and G" represents breakdown of the gel structure allowing the material to flow as a viscous liquid (liquid-like behaviour). The cross-over of G' and G" of the optimized mucoadhesive SRMS-based nano-lipogel was quite above 300 Pa, indicating that the formulation possesses a rigid nanostructure [21]. Before the cross-over, the value of loss tangent (tan $\delta = G''/G'$), which is a measure of the relative contribution of viscous components to the mechanical properties of the materials, was < 1 (phase angle, $\delta < 45$ °) for the optimized mucoadhesive SRMS-based nano-lipogel formulation when G' > G" (solid gel response) but was > 1 (phase angle, $\delta > 45$ °) for the formulation, after the cross-over, when G" > G' (liquid-like response). Thus, as phase angle became smaller, the elasticity of the formulation increased, while the viscous behavior was reduced. As expected, phase angle values were found to be higher for the optimized mucoadhesive SRMS-based nano-lipogel formulation at higher shear stresses. At cross-over of G' and G", the loss tangent was zero (phase angle, $\delta = 45$ °) [29].

Dynamic viscosity is described as the flow resistance of the sample in the structured state, originating as viscous or elastic flow resistance to oscillating movement [30]. The dynamic viscosity of the optimized mucoadhesive SRMS-based nano-lipogel formulation decreased with increasing shear stress, indicating a shear-thinning behavior and the administration of the formulation will be enhanced at higher shear stresses. A high viscosity at low shear stress makes the optimized mucoadhesive SRMS-based nano-lipogel formulation easier to stay along the oral mucosa. Furthermore, the higher value of dynamic viscosity means greater resistance to flow in the structured state [29]. The high dynamic viscosity value of the optimized mucoadhesive SRMS-based nano-lipogel (batch F_2 Gel) was due to its more consistent gel structure. The observed large dynamic viscosities of the optimized mucoadhesive SRMS-based nano-lipogel formulation at low oscillatory stresses are characteristic of viscoelastic systems [31].

CONCLUSIONS

In this study, phospholipid-modified beeswax-based mucoadhesive SRMS-based nano-lipogels made up of lipid nanoparticles in a gel base were formulated and evaluated for enhanced physicochemical performance. There was decreased crystallinity of the drug when incorporated in the phospholipid-modified beeswax-based matrix which was confirmed by DSC analysis. The SLNs had low polydispersity indices, within nanometer size range and possessed good physicochemical properties. The developed mucoadhesive SRMS-based nano-lipogels were spreadable, pseudoplastic and viscoelastic. FT-IR spectroscopy confirms components compatibility and their stability in the formulation. Thus, SRMS-based nano-lipogels using beeswax and P90H can be a novel nanoplatform for improved physicochemical performance of MN.

ACKNOWLEDGEMENTS

This work makes part of the doctoral activities of Franklin Chimaobi Kenechukwu. We thank

Phospholipid GmbH, Köln, Germany for providing Phospholipon ® 90H (P90H) used in this study. We also acknowledge Lubrizol Corporation, Ohio, United States of America for the kind gift of Noveon® (Polycarbophil) as well as the Institut für Pharmazeutische Technologie, Technische Universität Carolo-Wilhelmina zu Braunschweig, Braunschweig, Germany for the use of HAAKE ThermoRheoWin rheometer in their laboratory for the rheological study. This research received financial support from Tertiary Education Trust Fund (TETFund) (Grant no. TETFUND/DESS/NRF/STI/13/) by Government of Nigeria.

REFERENCES

1. Silva AC, Amaral MH, GonzálezMira E, Santos D, Ferreira D. Solid lipid nanoparticles (SLN)-based hydrogels as potential carriers for oral transmucosal delivery of Risperidone: preparation and characterization studies. *Colloids and Surfaces B: Biointerfaces.* 93, 2012: 241 – 248.
2. Shen C, Xu P, Shen B, Min H, Li X, Han J, Yuan H. Nanogel for dermal application of the triterpenoids isolated from *Ganoderma lucidum* (GLT) for frostbite treatment. *Drug Delivery*. 2014:1 – 9.
3. Soad AY, Omaima NE, Emad BB. Design and *in vitro*/*in vivo* evaluation of novel mucoadhesive buccal discs of an antifungal drug: relationship between swelling, erosion, and drug release. *American Association of Pharmaceutical Scientists Pharmaceutical Science and Technology.* 9, 2008:1207–1217.
4. Ramadan AA. Formulation and evaluation of bioadhesive gels containing miconazole nitrate. *Journal of Applied Scientific Research* 4, 2008:1052–1065.
5. Mazzarino L, Borsali R, Lemos-Senna E. Mucoadhesive films containing chitosan-coated nanoparticles: a new strategy for buccal curcumin release. *Pharmaceutical Nanotechnology* 103, 2014:3764–3771.
6. Almalik A, Donno R, Cadman CJ. Hyaluronic acid-coated chitosan nanoparticles: molecular weight-dependent effects on morphology and hyaluronic acid presentation. *Journal of Controlled Release*. 172, 2013:1142–1150.
7. Hembram KC, Prabha S, Chandra R. Advances in preparation and characterization of chitosan nanoparticles for therapeutics. *Artificial Cells Nanomedicine and Biotechnology*. 44, 2016:305–314.
8. Rençber S, Karavana SY, Yılmaz FF, Erac B, Nenni M, Özbal S, Pekçetin C, Gurer-Orhan H, Hoşgör-Limoncu M, Güneri P, Ertan G. Development, characterization and *in vivo* assessment of mucoadhesive nanoparticles containing fluconazole for the local treatment of oral candidiasis. *International Journal of Nanomedicine*. 11, 2016: 2641 – 2653.
9. Attama AA, Momoh MA, Builders, PF. Lipid nanoparticulate drug delivery systems: A revolution in dosage form design and development. In: A.D. Sezer (ed.), Recent Advances in Novel Drug Carrier Systems, InTech publishers, Rijeka, Croatia, 2012, pp. 107–140.
10. Chime SA, Onyishi IV. Lipid-based drug delivery systems (LDDS): Recent advances and applications of lipids in drug delivery. *African Journal of Pharmacy and Pharmacology*. 7, 2013:3034–3059.
11. Umeyor CE, Kenechukwu FC, Ogbonna JDN, Chime SA, Attama AA. Preparation of novel solid lipid microparticles loaded with gentamicin and its evaluation *in vitro* and *in vivo*. *Journal of Microencapsulation*. 29, 2012:296–307.
12. Kenechukwu FC, Momoh MA, Umeyor CE, Uronnachi EM, Attama AA. Investigation of novel solid lipid microparticles based on homolipids from *Bos indicus* for the delivery of gentamicin. *International Journal of Pharma Investigation.* 6, 2016:32–38.
13. Momoh MA, Esimone CO. Phospholipon 90H (P90H)-based PEGylated microscopic lipospheres delivery system for gentamicin: an antibiotic evaluation. *Asian Pacific Journal of Tropical Biomedicine* 2, 2012:889–94.
14. Attama AA, Umeyor CE. The use of solid lipid nanoparticles for sustained drug release. *Therapeutic Delivery*. 6, 2015:669–684.
15. Attama AA, Kenechukwu FC, Onuigbo EB, Nnamani PO, Obitte NC, Finke JH, Pretor S, Muller-Goymann CC. Solid lipid nanoparticles encapsulating a fluorescent marker (coumarin 6) and anti-malarials – artemether and lumefantrine: evaluation of cellular uptake and anti-malarial activity. *European Journal of Nanomedicine*. 2016:1 -10.
16. Kenechukwu FC, Momoh MA, Nnamani PO, Ogbonna JDN, Umeyor CE, Attama AA. Improved bioactivity of gentamicin from novel solid lipid microparticles based on beeswax. *Nigerian Journal of Pharmaceutical Research*. 10, 2014:35–45.
17. Wavikar P, Vavia P. Nanolipidgel for enhanced skin deposition and improved antifungal activity.

American Association of Pharmaceutical Scientists Pharmaceutical Science and Technology. 14, 2013:222–233.
18. Zhenqing HZ. Phytosomes loaded with mitomycin C-soybean phosphatidylcholine complex developed for drug delivery. *Molecular Pharmaceutics*. 10, 2013:90−101.
19. Xu S, Cavera VL, Rogers MA, Huang Q, Zubovskiy K, Chikindas ML. Benzoyl peroxide formulated polycarbophil/carbopol 934P hydrogel with selective antimicrobial activity, potentially beneficial for treatment and prevention of bacterial vaginosis. *Infectious Disease and Obstetrics Gynecology*. 2013:1–10.
20. Nnamani PO, Kenechukwu FC, Dibua EU, Ogbonna CC, Monemeh UL, Attama AA. Transdermal microgels of gentamicin. *European Journal of Pharmaceutics and Biopharmaceutics*. 84, 2013:345–354.
21. Rossi S, Maricello M, Bonferoni MC, Ferrari F, Sandri G, Dacarro C. Thermally sensitive gels based on chitosan derivatives for the treatment of oral mucositis. *European Journal of Pharmaceutics and Biopharmaceutics* 17, 2010:360-365.
22. Attama AA, Schicke BC, Müller-Goymann CC. Further characterization of theobroma oil beeswax admixtures as lipid matrices for improved drug delivery systems. *European Journal of Pharmaceutics and Biopharmaceutics* 64, 2006:294–306.
23. Tsutsumi S, Iida M, Tada N. Characterization and evaluation of miconazole salts and cocrystals for improved physicochemical properties. *International Journal of Pharmaceutics*. 421, 2011:230–236.
24. Bhalekar MR, Pokharkar V, Madgulkar A, Patil N. Preparation and evaluation of miconazole nitrate-loaded solid lipid nanoparticles for topical delivery. *American Association of Pharmaceutical Scientists Pharmaceutical Science and Technology*.10, 2009:289–296.
25. Cerdeira AM, Mazzotti M, Gander B. Miconazole nanosuspensions: influence of formulation variables on particle size reduction and physical stability. *International Journal of Pharmaceutics.* 396, 2010:210–218.
26. Attama AA, Reichl S, Müller-Goymann CC. Diclofenac sodium delivery to the eye: *in vitro* evaluation of novel solid lipid nanoparticle formulations using human cornea construct. *International Journal of Pharmaceutics*. 355, 2008:307–313.
27. Attama AA, Schicke BC, Paepenmüller T, Müller-Goymann CC. Solid lipid nanoparticulate dispersions containing mixed lipid core and a polar heterolipid: characterization. *European Journal of Pharmaceutics and Biopharmaceutics*. 67, 2007:48–57.
28. McCarron PA, Donnely RF, Canning PE, McGovern JG, Jones DS. Bioadhesive, non-drug-loaded nanoparticles as modulators of candidal adherence to buccal epithelial cells: a potentially novel prophylaxis for candidiasis. *Biomaterials* 25, 2004: 2399 – 2407.
29. Sabri LA, Sulayman HT, Khalil YI. An investigation of release and rheological properties of miconazole nitrate from emulgel. *Iraqi Journal of Pharmaceutical Science*. 18, 2009:26–31.
30. Karavana SY, Rencber S, Senyigit ZA, Baloglu E. A new *in situ* gel formulation of itraconazole for vaginal administration. *Pharmacology and Pharmacy*. 3, 2012:417–426.
31. Chen J, Zhou R, Li L, Li B, Zhang X, Su J. Mechanical, rheological and release behaviors of a poloxamer 407/poloxamer 188/carbopol 940 thermosensitive composite hydrogel. *Molecules*. 18, 2013:12415–12425.